Role of superposition of dislocation avalanches in the statistics of acoustic emission during plastic deformation

M. A. Lebyodkin,[1,*] I. V. Shashkov,[1,2] T. A. Lebedkina,[2] K. Mathis,[3] P. Dobron,[3] and F. Chmelik[3]
[1]*Laboratoire d'Etude des Microstructures et de Mécanique des Matériaux, LEM3, CNRS/Université de Lorraine, UMR 7239, Ile du Saulcy, 57045 Metz, France*
[2]*Institute of Solid State Physics, Russian Academy of Sciences, 142432 Chernogolovka, Russia*
[3]*Department of Physics of Materials, Charles University, Ke Karlovu 5, CZ-121 16 Prague 2, Czech Republic*
(Received 23 July 2013; published 9 October 2013)

Various dynamical systems with many degrees of freedom display avalanche dynamics, which is characterized by scale invariance reflected in power-law statistics. The superposition of avalanche processes in real systems driven at a finite velocity may influence the experimental determination of the underlying power law. The present paper reports results of an investigation of this effect using the example of acoustic emission (AE) accompanying plastic deformation of crystals. Indeed, recent studies of AE did not only prove that the dynamics of crystal defects obeys power-law statistics, but also led to a hypothesis of universality of the scaling law. We examine the sensitivity of the apparent statistics of AE to the parameters applied to individualize AE events. Two different alloys, MgZr and AlMg, both displaying strong AE but characterized by different plasticity mechanisms, are investigated. It is shown that the power-law indices display a good robustness in wide ranges of parameters even in the conditions leading to very strong superposition of AE events, although some deviations from the persistent values are also detected. The totality of the results confirms the scale-invariant character of deformation processes on the scale relevant to AE, but uncovers essential differences between the power-law exponents found for two kinds of alloys.

DOI: 10.1103/PhysRevE.88.042402 PACS number(s): 62.20.F−, 62.65.+k, 89.75.Da, 89.75.Fb

I. INTRODUCTION

Extended dynamical systems characterized by jerky response to slowly changing external force are known to be prone to avalanchelike behavior, reflected in power-law statistical distributions of magnitudes and durations of avalanches. Well-known examples in physics and material science include the Barkhausen noise in magnetic materials [1], vortex avalanches in superconductors [2], charge density waves [3], fracture [4], martensitic transformations [5], dry friction [6], earthquakes [7], discontinuous plastic flow [8–10], fatigue dynamics [11], and so on.

Recent investigations of plastic deformation regarding intermediate scales between the microscopic scale of individual crystal defects and the macroscopic scale of a bulk specimen, revealed a ubiquitous character of avalanchelike behavior in the system of crystal defects. In particular, power-law distributions $p(E) \sim E^{-\beta}$ of acoustic energy E were found for acoustic emission (AE) accompanying macroscopically smooth plastic flow controlled by dislocation glide [12,13], mechanical twinning [14], and the Portevin-Le Chatelier (PLC) effect, a macroscopic plastic instability caused by interaction of dislocations with solute atoms [15,16]. Such observations led to a conclusion on an inherently intermittent critical-like nature of the collective dynamics of defects [17]. Moreover, investigation of AE in various pure single crystals yielded rather close values of β for dislocation glide and twinning, approximately bounded in a range of 1.5 to 2. They also occurred to be similar to β values characterizing plastic strain jumps during deformation of micropillars of various materials (e.g., Ref. [18]).

These results gave rise to a hypothesis of universality of the scaling law describing plasticity processes on a mesoscopic scale. However, investigation on polycrystalline ice yielded a lower β value (about 1.35), which was conjecturally attributed to the development of more powerful AE events through triggering of avalanches in the neighboring polycrystalline grains [19]. On the other hand, significantly larger β values, varying between 2 and 3 and depending on the strain and strain rate, were found for the PLC effect [15,16,20]. In this case, merging of acoustic events, resulting in drastic bursts in the recorded durations (but not amplitudes), was experimentally observed at the moments of stress drops caused by the plastic instability at not very high strain rates. As suggested in these papers, such behavior is akin to the phenomenon of synchronization in extended dynamical systems [21]. One consequence of this effect is that the statistics of durations of AE events cannot be clearly quantified in terms of a power law. It should be noted that besides this difficulty caused by a particular physical mechanism, the measurement of durations generally suffers from various artifacts, such as sound reflections, wave modulation by the propagating medium, and so on. On the contrary, not only was clear power-law behavior found for AE amplitudes, but the detected exponents were almost independent of the criteria commonly applied to individualize AE events (see Sec. II).

These observations renew a general question of how the possible overlap of the analyzed events can affect the results of the statistical analysis of experimental data. Understanding this issue is essential for careful determination of critical exponents and relationships between them and, therefore, for selection of theoretical models relevant to the phenomena studied. Various models were proposed in the literature to explain scale-free statistics, including the concept of self-organized criticality (SOC), which considers systems spontaneously reaching a

*Corresponding author: mikhail.lebedkin@univ-lorraine.fr

critical state without fine tuning of an order parameter [22], the models taking into account fluctuations near the critical point [23] or the slow sweeping of a control parameter [24], etc. All theoretical models make use of a common suggestion of a very slow driving rate or, in the ideal case, interrupted loading during the propagation of an avalanche. This condition makes it possible to avoid simultaneous propagation of two or more avalanches. The experimental conditions are often far from this ideal situation, so that avalanches may overlap in time and in space and be recorded as a single event.

Several works concerned a possible effect of the driving rate on the critical exponents. In the pioneering theoretical paper [25], the mean-field exponents for the amplitude S and duration τ of Barkhausen jumps in soft ferromagnetic materials were predicted to decrease linearly with the field driving rate. The relevant experiments [26] led to distinguishing two cases: (i) when the exponent β_τ describing the avalanche duration probability tends to 2 for zero rate of the external magnetic field, such material shows a linear decrease in β_S and β_τ with an increase in the field rate; (ii) in the case when β_τ (0) < 2, the slopes are independent of the field rate. In Ref. [27] a theoretical explanation of such behavior was proposed through consideration of a linear superposition of avalanches. According to this model, the decrease in the slopes of the power-law dependencies in the former case occurs because small events are absorbed into larger ones. On the contrary, no changes are observed when the rate is varied in the latter case, because the superposition is already strong at very low field rates. The authors also analyzed theoretically the case $\beta_\tau > 2$ and found that the exponents must be rate independent for small enough rates, but a crossover to one-dimensional percolation on the time axis should occur when the rate is increased. It should be noted that the above cases do not exhaust experimental observations. So, logarithmic dependencies on the cooling rate were observed for amplitude distributions of AE signals accompanying martensitic transformations [28].

Investigations of this question in plasticity have not been undertaken until recently [16,29]. One of the reasons for this deficiency is that besides the above-mentioned difficulties concerning the measurement of time characteristics of AE, such investigations represent a fundamental problem: Deformation behavior is never statistically stationary because of the microstructure changes, which are actually at the origin of the work hardening of the material. As a result, the values of the critical exponents may evolve during deformation. Moreover, there exist no two samples with identical microstructure, and besides, the microstructure evolution depends on various factors including the strain rate. Therefore, a rigorous comparison of the results obtained at different strain rates is hardly possible.

To study the effect of overlapping, we adopted another strategy, which became possible due to recent development of the data streaming technique for AE measurements [30]. It allows continuously storing an entire AE signal generated during a test, instead of the traditional method of keeping only the measurements of several characteristics of AE events detected in real time using some preset criteria. By varying the event individualization criteria, various sets of events can then be extracted from the same recorded signal and analyzed.

The experiments were performed on MgZr and AlMg alloys. The plastic deformation of both materials is accompanied by strong acoustic activity but controlled by different microscopic mechanisms: a combination of twinning and dislocation glide in hexagonal MgZr alloys and the PLC effect in face-centered cubic AlMg alloys. These materials present a particular interest for the analysis because both the wave forms of the individual acoustic events and overall AE behavior have different signatures in the case of twinning or dislocation glide [14,31]. An additional interest in the investigation of the PLC effect is due to its intricate spatiotemporal behavior, associated with repetitive strain localization in deformation bands and concomitant stress serrations. According to traditional nomenclature, three types of the PLC effect corresponding to virtually random nucleation of deformation bands at low strain rates (type C), hopping of deformation band at intermediate strain rates (type B) and their quasicontinuous propagation at high strain rates (type A) are generally distinguished [32]. The serrated deformation curves were found to carry signatures of SOC for type A behavior [10,33] and deterministic chaos [34] for type B behavior [35,36]. It is noteworthy that although AE always obeys power laws, the stress serrations demonstrate distributions with characteristic peaks for type C and type B behaviors.

II. EXPERIMENTAL TECHNIQUE AND DATA PROCESSING

Flat tensile specimens with a typical dog-bone shape and $30 \times 7 \times 1$ mm^3 gauge part were cut from a cold-rolled sheet of a polycrystalline Al-5 wt% Mg alloy with the average grain size about 4–6 μm and tested either in as-rolled conditions or after annealing for 2 h at 400 °C followed by water quenching. Such heat treatment, which was aimed at dissolving second-phase inclusions and producing a virtually homogeneous solid solution [37], also led to partial recrystallization and resulted in grain size about twice as large. MgZr specimens with 5×5 mm^2 cross section and 25-mm gauge length were prepared from as-cast material and annealed for 1 h at 250 °C. Materials with several compositions were used, taking into account that variation of Zr content strongly modifies the grain size. The samples with 0.04 wt%, 0.15 wt%, and 0.35 wt% of Zr had the average grain size of 550, 360, and 170 μm, respectively.

All samples were deformed by tension at room temperature and a constant crosshead speed. As said in the Introduction, the PLC effect displays various types of behavior depending on the imposed strain rate. For this reason, AlMg samples were deformed in a wide range of applied strain rate, $\dot{\varepsilon}_a = 2 \times 10^{-5}$ s^{-1} $- 2 \times 10^{-2}$ s^{-1}, where the indicated values correspond to the initial specimen length. Since the continuous recording of AE results in huge data files, the entire data stream was gathered only for high enough strain rates, $\dot{\varepsilon}_a > 2 \times 10^{-4}$ s^{-1}. The AE signal was recorded piecewise in the slower tests. MgZr samples were tested at $\dot{\varepsilon}_a = 3.5 \times 10^{-4}$ s^{-1}.

The AE was captured by a piezoelectric transducer clamped to the specimen surface near its upper end using silicon grease and a spring, preamplified and recorded on a linear scale (mV) at a sampling rate of 1 or 2 MHz with the aid of the Euro Physical Acoustics system. The experiments on AlMg

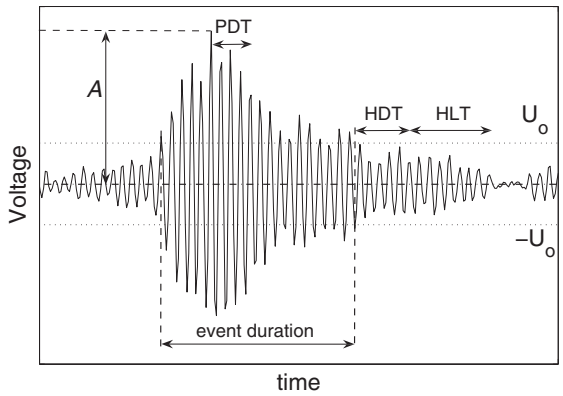

FIG. 1. Scheme illustrating the selection of an individual AE event and definition of its peak amplitude A.

alloys were done using a Micro-80 sensor with the operating frequency band 200–900 kHz, fixed to the wide specimen head above its gauge length. In the experiments on Mg alloys, a miniaturized MST8S transducer (3 mm diameter, frequency band from 50 to 600 kHz) was used. This precaution was taken to warrant a good acoustic contact if the specimen surface is distorted during deformation.

The individualization of AE events in the data stream mimicked one of the standard procedures implemented in acoustic systems to extract acoustic events ("hits") in real time by application of some preset criteria, without recording the entire AE signal. Namely, the software reads the recorded data line after line and detects the crossings of a threshold voltage U_0, as represented in Fig. 1. An event is considered to start when the signal surpasses U_0. Its end is detected when the signal remains below U_0 for a period exceeding a hit definition time (HDT), designated in the formulae below as $t_H D$. Afterwards, no measurements are performed during the hit lockout time (HLT), or "dead time," in order to filter out sound reflections. To determine the event peak amplitude A, the software detects local maxima and compares them to the absolute maximum detected so far. The latter is recorded as the event peak amplitude if it was not exceeded during the so-called peak definition time (PDT). Otherwise, it is assigned the new value and the time counting is restarted. In what follows, PDT is supposed to be equal to half HDT, if not stated explicitly otherwise.

Statistical distributions of the squared amplitude A^2 were studied in the present work, following the approach suggested in Ref. [12] and based on a suggestion that this quantity reflects the energy dissipated by viscoplastic deformation during acoustic events. As explained in the Introduction (see also [16] for more details), the analysis of durations and related characteristics, such as energy obtained by the signal integration, is delicate in the presence of plastic instability and goes beyond the scope of the present paper. Discrete frequency distributions [38] of the values of A^2 were calculated using linear bins, similar to our previous works [10,16]. The statistical samples composed of at least 350 to tens of thousands of hits depending on the deformation conditions and hit individualization parameters. To handle the statistics of rare large events, the method of variable bin sizes was used. Hence, when an initial-size bin contained less than a preset minimum number of events, it was merged with the next bins until this minimum number (5 in the present work) was reached. The obtained numbers were then normalized by the bin sizes (cf. [10]). The slope of the resulting dependence $P(A^2)$ in double logarithmic coordinates, yielding the corresponding power-law exponent, and the error of its determination were calculated using the least-squares method. The detection of straight intervals was direct because in most cases, the present data did not manifest a cutoff (cf. [16,20]). Recently, a new generalized method, based on the Monte Carlo technique, was proposed to evaluate the closeness of experimental statistics to a power law [39]. The test calculations showed that the evaluation of the exponent and its uncertainty by these two methods provided similar results in our case.

It should be underlined that the power-law distributions calculated for AE events extracted from the data stream practically coincide with the dependencies obtained for events extracted by the acoustic device in the real time, although the data streaming yields data on a linear scale, while the standard device output is in the logarithmic (decibel) scale (cf. [29]).

III. EXPERIMENTAL RESULTS AND DISCUSSION

The overall AE pattern observed for both alloys is similar to the literature data on various materials [40]. Namely, AE occurs practically from the beginning of the test, during macroscopically elastic deformation, reaches a high intensity in the region of the elastoplastic transition, and then decreases in intensity and displays a long enough quasistationary period, when the average AE amplitude does not vary considerably. This close-to-steady behavior usually lasts until the onset of necking, providing enough data for the statistical analysis.

Figure 2 represents examples of AE signals observed for two investigated alloys. It can be recognized that their shapes correspond to qualitatively different situations. In the case of MgZr alloys, the signal displays series of well-separated hits, as often reported for twinning [40]. In contrast, the AlMg alloy is characterized by closely following events, so that the extraction of individual hits is less unambiguous.

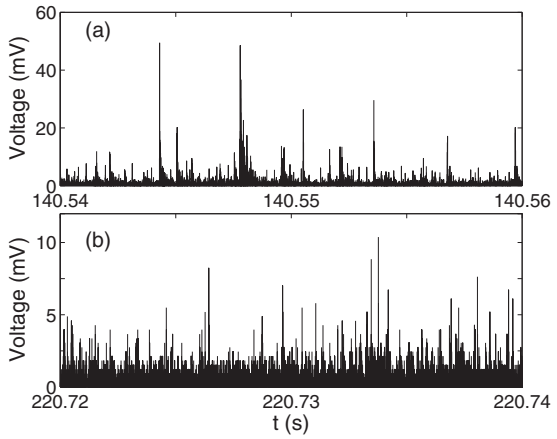

FIG. 2. Examples of continuously recorded AE signals. (a) Mg0.35wt%Zr sample deformed at $\dot{\varepsilon}_a = 3.5 \times 10^{-4}$ s^{-1}; (b) Al5wt%Mg sample deformed at $\dot{\varepsilon}_a = 2 \times 10^{-4}$ s^{-1}. It should be noted that the voltage values are given for illustration but cannot be used for comparison of the signal intensity because of the use of different experimental setups in the tests on two kinds of alloys.

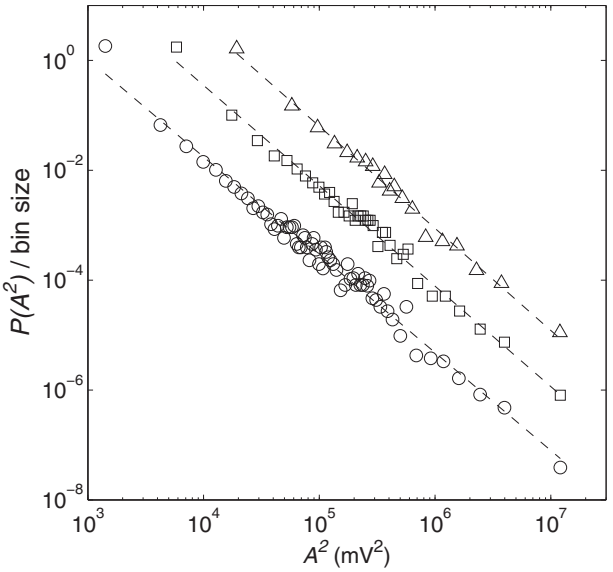

FIG. 3. Effect of the voltage threshold on the probability density of squared amplitudes of AE events for the same specimen as in Fig. 2(a). Circles, $U_0 = 9$ mV, $\beta = 1.80 \pm 0.02$; squares, $U_0 = 24.4$ mV, 1.83 ± 0.04; triangles, $U_0 = 60.1$ mV, 1.87 ± 0.05.

These observations justify the choice of the materials for investigation, representing two distinct cases.

A. MgZr alloys

Figure 3 illustrates that for an appropriate choice of parameters, MgZr alloy displays power-law distributions of A^2 over a range as long as four orders of magnitude (curve 1). This figure also represents the effect of U_0 on the extent and slope of the power-law probability functions for one choice of time parameters. It can be recognized that the slope is very robust and changes only slightly, from $\beta = 1.80 \pm 0.02$ to $\beta = 1.87 \pm 0.05$, when U_0 is varied from 9 to 60.1 mV. The main effect of the increase in U_0 consists of the impoverishment of the statistical sample because of the truncation of low-amplitude events, and the resulting cutoff of the left-hand part of the scaling interval.

The summary of the results of such calculations is presented in Fig. 4. It shows β dependencies on all three parameters, U_0, HDT, and HLT, and for all three kinds of MgZr alloys. Figure 4(a) represents such dependencies for fixed time parameters and U_0 varied in a range from 4.5 to 90 mV, above which the amount of data becomes too small for the statistical analysis. Besides, an additional $\beta(U_0)$ curve is traced using another choice of HDT for the same Mg0.35%Zr sample, in order to illustrate the effect of HDT on the entire $\beta(U_0)$ dependence. This representation completes the data on β vs HDT dependencies which are traced for fixed U_0 and HLT in Fig. 4(b). A similar manner to illustrate the effect of various parameters was adopted in all three parts of Fig. 4.

The data of Fig. 4(a) testify that, in agreement with the above discussion of the examples shown in Fig. 3, β grows with increasing U_0 but the observed changes are not strong. The overall variation does not exceed 0.2. Moreover, the main changes occur in a narrow range (about one-tenth of the total U_0 range) and then saturate, so that further variations are

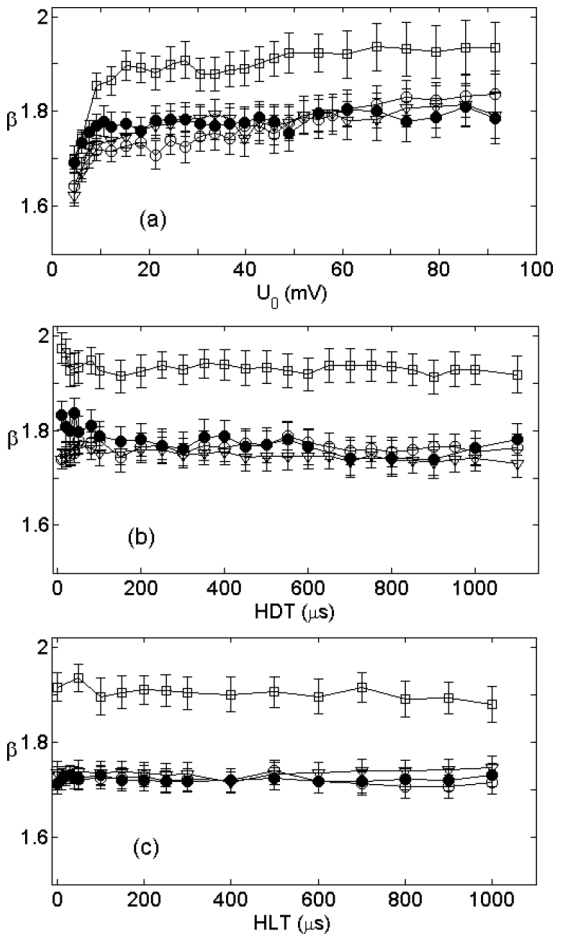

FIG. 4. Effect of (a) U_0, (b) HDT, and (c) HLT settings on the power-law index β for MgZr specimens deformed at $\dot{\varepsilon}_a = 3.5 \times 10^{-4}$ s^{-1}. Open and solid circles, Mg0.35%Zr; triangles, Mg0.15%Zr; squares, Mg0.04%Zr. (a) HLT = 100 μs and HDT = 800 μs, except for the case of solid circles corresponding to HDT = 50 μs. (b) HLT = 0 μs and $U_0 = 17$ mV; solid circles, $U_0 = 67$ mV. (c) $U_0 = 17$ mV and HDT = 100 μs; solid circles, HDT = 20 μs.

either weak or indiscernible against the experimental error. The faster initial changes can be easily explained by taking into account that AE signals always contain a continuous background, which may be caused not only by the inevitable experimental noise but also by the so-called continuous AE, which is believed to be produced by less correlated motions of dislocations. In the extreme case when U_0 is taken lower than the minimum background level, all AE events will be merged via this "go between" and the entire AE record will be determined as a single avalanche. It is evident from this consideration that the low β values observed for the low thresholds U_0 can be explained by the merging of successive AE events, so that the number of smaller events is decreased and the apparent power law is flatter than the true one. The end of the fast changes in β can be explained by U_0 exceeding the continuous background level, so that the AE events become essentially isolated. The further slight (if any) evolution of β with increasing U_0 may be attributed to the reduction in the remaining weak overlapping.

This suggestion is confirmed by the comparison of the curves shown in Fig. 4(a) for two values of HDT. Indeed,

the degree of overlapping must depend on the relationships between all identification parameters and the temporal arrangement (clustering) of AE hits. For example, the reduction in HDT must improve the individualization of AE events at a given U_0. Consequently, the $\beta(U_0)$ dependence must saturate quicker. This is indeed observed, as illustrated in Fig. 4(a). Importantly, the effect of the voltage threshold is insignificant in a wide U_0 range for all HDT values. Finally, it is worth noting that the weak dependencies detected for larger U_0 values may be due not only to residual merging of AE events but perhaps also to biasing because of the statistics depletion.

Another proof for the above consideration is provided by the data for the large-grain Mg0.04%Zr alloy. Indeed, although considerably higher β values are found for these samples, the shape of the $\beta(U_0)$ dependence observed is similar to that for other alloys, so that the entire dependence is simply shifted upwards. This observation testifies that the mechanism of the U_0 effect on β must be independent of the material, as suggested above.

The influence of the time parameters was found to be even weaker with regard to that of the voltage threshold. Figure 4(b) represents the effect of HDT variation in the range from 10 to 1100 μs for two threshold levels: one selected just above the range of the sharp $\beta(U_0)$ dependence (17 mV) and another taken in the far saturation region (67 mV). The HLT was deliberately taken to be zero, in order to make the effect of other parameters more pronounced, although such a choice is never made in practice. In spite of these efforts, it can be seen that the effect of HDT is virtually indistinguishable for both choices of the threshold, except for some weak increase in β that can be discerned in a narrow range of low HDT values (below 50 μs) for $U_0 = 67$ mV. The latter observation is not surprising because taking a small HDT may result in recording the sound reflections following an AE event as independent hits and therefore lead to an apparent increase of the number of "events" with lower amplitudes. Therewith, this effect manifests itself only for the higher threshold, i.e., when the statistical sample is depleted.

Finally, Fig. 4(c) represents the results of a similar analysis for HLT. It can be expected that its possible effect must be due to the statistics impoverishment because the "dead time" results in a loss of a part of information contained in the signal. Such loss of information must not affect the power-law exponent in the ideal case of perfect scale-invariant and unlimited statistical sample, but may manifest itself for real signals. The data shown in Fig. 4(c) prove that no significant dependence of the power law on HLT was found over the whole studied range from 0 to 1 ms. The entirety of the above results testifies that the power laws observed for MgZr alloys are robust with regard to the criteria used to select the AE events.

Finally, all three figures prove that the material with a large grain size is characterized by higher β values, in conformity with the literature data presented in Sec. I. It should also be noted that it is not a sole example of the influence of the microstructure on the underlying power law. In particular, although β values found for MgZr (Fig. 4) are close to those reported for various pure hexagonal materials [12–14,19], still they are systematically higher than the typical values of 1.5 to 1.7 given in these papers. Another example is provided by the data on AlMg alloy presented in the next section.

B. AlMg alloy

The data obtained on AlMg represent a qualitatively different case because of the strong overlapping and merging of neighboring AE hits, as illustrated in Fig. 2 (cf. [16,20]). Besides, the AE has a lower intensity than during twinning of MgZr alloys and, therefore, a lower signal-to-noise ratio. Figure 5 summarizes the results of the analysis for as-delivered and annealed AlMg specimens deformed at different strain rates corresponding to three distinct types of behavior of the PLC effect. It can be seen that the influence of the identification parameters is stronger than in the case of MgZr alloys and the dependencies are less monotonous. It is obvious that because of the effects of merge of AE events, the results might depend on various factors, such as the specific relationships between the selected time and voltage parameters, the level of the measurement noise, and the distribution of the on-off time periods in the AE signal, which reflects the distribution of the hits durations and their occurrence times. Therefore, we only stop on some characteristic trends.

First of all, it is worth noting that the β range found for the AlMg alloy (typically from 2 to 3) lies remarkably above the similar range for MgZr alloys (1.5 to 2). This difference is much more significant than any variation in β observed upon modification of the events identification criteria. Furthermore, β values are almost always lower for the as-delivered specimens (circles) than for the annealed ones (squares). Taking into account that annealing leads to an increase in the average grain size, this observation is consistent with the above-mentioned grain-size effect observed for MgZr alloys. Importantly, the change in β upon annealing is usually more significant than the uncertainty of β determination caused by the influence of the identification criteria.

More specifically, the first row of Fig. 5 represents $\beta(U_0)$ dependencies. For the high strain rate [Fig. 5(a)] and large HDT and HLT values (solid lines), β displays behavior similar to the case of Mg alloys, namely a fast initial rise followed by almost no dependence. The fast initial change, attributed in the previous section to the amalgamation of successive AE events by the agency of the continuous background, disappears when HDT is reduced, so that β becomes nearly constant in the entire U_0 range. It is natural to suppose that when the imposed strain rate is decreased, the measurable AE events requiring the motion of powerful enough dislocation ensembles become rarer and better separated (the on-off time ratio becomes larger).[1] As a result, the fast initial change does not occur for lower $\dot{\varepsilon}_a$ [Figs. 5(b) and 5(c)]. The $\beta(U_0)$ dependencies obtained for the lowest $\dot{\varepsilon}_a$ [Fig. 5(c)] using a large HDT show a somewhat opposite tendency: a slow descent with increasing U_0. This trend is also consistent with the discussed framework. Indeed, the increase in U_0 leads to discarding small events and decaying big compound events into two or more (big) components, thus resulting in a larger fraction of big events and

[1]The experimental observations explicitly confirming this expectation were described in detail in Ref. [20].

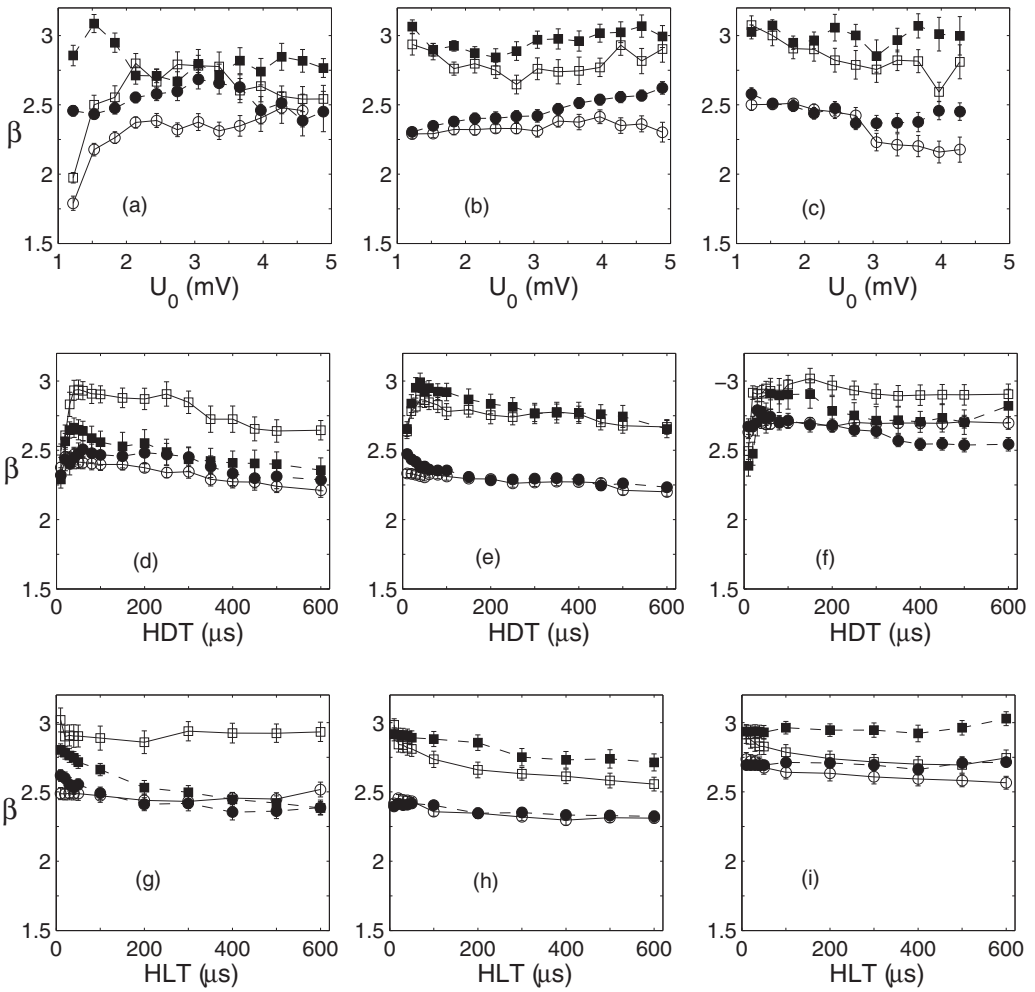

FIG. 5. Effects of U_0, HDT, and HLT parameters on the power-law index β for AlMg specimens deformed at (left column) $\dot{\varepsilon}_a = 6 \times 10^{-3}$ s^{-1}; (middle column) $\dot{\varepsilon}_a = 2 \times 10^{-4}$ s^{-1}; (right column) $\dot{\varepsilon}_a = 2 \times 10^{-5}$ s^{-1}. Circles and squares designate as-delivered and annealed specimens, respectively; solid and dashed lines designate parameters which are kept constant. (Top row) Solid lines, HDT = 300 μs, HLT = 300 μs; dashed lines, HDT = 30 μs, HLT = 100 μs; (middle row) solid lines, $U_0 = 1.85$ mV; dashed lines, $U_0 = 3.4$ mV (HLT = 300 μs); (bottom row) solid lines, HDT = 10 μs; dashed lines, HDT = 50 μs ($U_0 = 1.85$ mV).

an apparently lower β value. This effect is illustrated in Fig. 6, which demonstrates the change in the slope of the power law for a truncated distribution. It should be noted that alongside the left truncation, obviously stemming from scrapping small hits, some truncation from the right is also seen. It is a common effect for a limited observation time, because the large events are rare and their occasional loss within the dead-time intervals may lead to some variation of the right distribution boundary when these intervals are reorganized. The companion curves in Fig. 5(c) display the behavior for a reduced value of HDT and demonstrate that the decreasing trend in $\beta(U_0)$ dependencies is suppressed when the AE events are better separated due to a lower HDT. In this case, the increase in U_0 leads only to (left) truncation without renormalizing the slope of the power-law dependence. It should also be noted from this point of view that in all three panels [(a)–(c)] the $\beta(U_0)$ dependencies corresponding to higher HDT (solid lines) generally lie below their homolog for a lower HDT (dashed lines), in conformity with the discussed influence of the AE events merging on the seeming β value.

The above data prove that the choice of the time parameters can be quite important and entrain noticeable changes in the power-law exponents. The β vs HDT dependencies are displayed in the second row of Fig. 5. It is noteworthy that, as illustrated in Figs. 5(a) and 5(d) for the high strain rate, choosing a small U_0 value corresponding to the range of fast changes on the $\beta(U_0)$ dependence may lead to a considerable shift of the β vs HDT curve with regard to its counterpart for a higher U_0 value. Such a shift is observed for the annealed sample [Fig. 5(d), squares]. The difference is inessential, though, for the as-delivered sample. It is also weak for the low strain rate and practically negligible for the intermediate strain rate which is characterized by weak $\beta(U_0)$ dependencies.

In spite of these quantitative changes, similar shapes of the β vs HDT curves are obtained for all three strain rates. First, β rapidly increases approximately by 0.2 with increasing HDT from 10 to 40 μs, then it slowly reduces. The initial fast rise may be absent, as illustrated by two upper curves in Fig. 5(e), which correspond to an as-delivered sample deformed at $\dot{\varepsilon}_a = 2 \times 10^{-4}$ s^{-1}. This rise can be explained

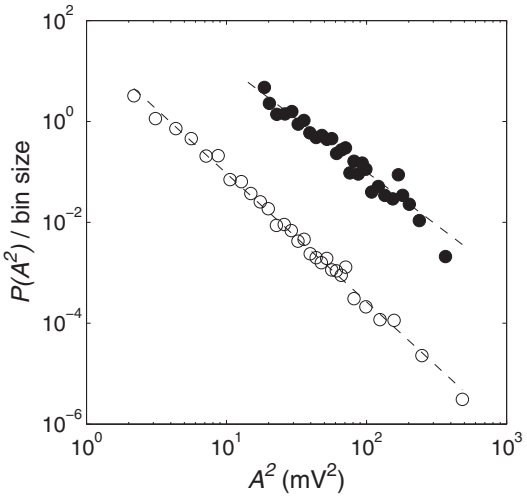

FIG. 6. Effect of the voltage threshold on the amplitude statistics of AE events for the AlMg specimen designated by the open circles and solid line in Fig. 5(c). Open circles, $U_0 = 1.22$ mV, $\beta = 2.54 \pm 0.04$; solid circles, $U_0 = 4.27$ mV, $\beta = 2.0 \pm 0.1$.

if one takes into account that the small HDT may lead to erroneously taking for the event's peak amplitude one of its first local maxima. This error would enhance the fraction of small events and raise β correspondingly. It can be noticed that the strongest variations on the β vs HDT curves obtained for MgZr alloys were observed in the same HDT range [see Fig. 4(b)]. This observation justifies the value of 30–40 μs often recommended as the lower limit for selecting HDT in the investigation of plastic deformation of metals. The following descent of β, more significant for the higher strain rates, is obviously due to the above-discussed effect of AE events merging. The optimum HDT value does not seem to be the same for each strain rate. However, as the β dependencies are rather weak above HDT $= 40$ μs, this influence can be neglected in most cases.

The third row of Fig. 5 illustrates the effect of HLT for two choices of HDT. As could be expected, the power-law exponent relatively strongly depends on HLT for small HDT values, thus confirming the above discussion of the effect of HDT. However, for HDT $\geqslant 50$ μs, the influence of HLT is insignificant, similar to the data for MgZr. Its effect consists mostly of the statistics impoverishment which should not influence on the scale-invariant distributions, provided that enough data remain in the dataset.

IV. CONCLUSIONS

The effect of the superposition of avalanches on the experimental determination of the underlying power-law statistics was studied in the present work using the example of acoustic emission generated during plastic deformation of MgZr and AlMg alloys. It is proven that the criteria used to identify AE events only weakly influence on the apparent value of the power-law exponent β, as compared with the differences between β values either for two kinds of alloys or for the same material in which the grain size was modified. More specifically, the variations in β caused by the variation of the identification parameters are typically bounded in a range of several tenths, which is much narrower than the gap about 1 to 1.5 between β values obtained for AlMg and MgZr alloys.

In particular, a very weak influence is detected for Mg alloys, in consistence with the literature data reporting well-separated abrupt AE hits accompanying mechanical twinning. Indeed, almost no effect was discerned when HDT and HLT were varied. Somewhat stronger, albeit weak, effect is observed in a wide range of the voltage threshold U_0. The only case when a relatively strong influence on the power law is found corresponds to a narrow range of the lowest U_0 values and is most likely due to connection of successive AE events by mean of the continuous background. It is interesting that a similar effect of amplitude thresholding was observed very recently in compression of a porous silica ceramics deformed by multifragmentation [41]. Moreover, theoretical studies of the effect of thresholding did not reveal any effect on the amplitude distributions, although a strong influence was predicted for temporal avalanche statistics [42].

A somewhat less favorable situation for the application of the AE method is found under conditions of the PLC effect which is known to generate lasting AE events, most likely due to the merging of many hits because of successive triggering of many dislocation ensembles. Nevertheless, even in this case the influence of the event identification parameters is rather weak in wide ranges of parameters. The experiments on AlMg also make it possible to compare the data obtained in similar strain intervals and the same choice of individualization parameters but for different strain rates (see Fig. 5). This comparison reveals some tendency to an increase in β with decreasing $\dot{\varepsilon}_a$. It qualitatively agrees with the influence of the rate of change of the magnetizing field on the power-law statistics of the Barkhausen effect [26], as well as with theoretical predictions of the role of the driving rate [25,27]. It should be underlined, however, that the avalanche overlapping does not only depend on the driving rate but is a complex result of the action of various factors, including the noise level and the parameters used to extract avalanches.

The robustness of the avalanche statistics regarding their overlap made it possible to confirm the hypothesis that the plastic deformation manifests a universal avalanche-type nature on the scale relevant to AE, reflected in the scale-invariant character of the distribution of AE amplitudes (cf. [13–15,19]). However, it is shown that the power-law exponents do not take on a universal value for all microscopic mechanisms of plastic flow. Moreover, they show sensitivity to the microstructure, e.g., grain size, under conditions of action of the same mechanism.

ACKNOWLEDGMENTS

This work was supported by the French State through the program "Investment in the future" operated by the National Research Agency (ANR) and referenced by Grant No. ANR-11-LABX-0008-01 (LabEx DAMAS). It also received support from the Centre National de la Recherche Scientifique (exchange program between the CNRS and Russian Academy of Sciences, Grant No. EDC25170), as well as from the French Ministry of Foreign Affairs and the Ministry of Education, Youth and Sports of the Czech Republic, within the framework of the mobility program Contact-Barrande MEB

021004 (21971TH). K. Mathis, P. Dobron, and F. Chmelik gratefully acknowledge financial support from Research Grant No. P108/11/1267 financed by the Czech Science Foundation. P. Dobron is also grateful to the Charles University Research Center "Physics of Condensed Matter and Functional Materials" for financial support.

[1] P. J. Cote and L. V. Meisel, Phys. Rev. Lett. **67**, 1334 (1991).
[2] E. V. Matizen, S. M. Ishikaev, and V. A. Oboznov, J. Exp. Theor. Phys. **99**, 1065 (2004).
[3] P. A. Lee and T. M. Rice, Phys. Rev. B **19**, 3970 (1979).
[4] J. Aué and J. T. M. de Hosson, J. Mater. Sci. **33**, 5455 (1998).
[5] E. Vives, J. Ortín, L. Mañosa, I. Ràfols, R. Pérez-Magrané, and A. Planes, Phys. Rev. Lett. **72**, 1694 (1994).
[6] J. M. Carlson, J. S. Langer, and B. E. Shaw, Rev. Mod. Phys. **66**, 657 (1994).
[7] B. Gutenberg and C. F. Richter, Ann. Geofis. **9**, 1 (1956).
[8] V. S. Bobrov and M. A. Lebedkin, Fiz. Tverd. Tela **31**, 120 (1989) [Sov. Phys. Solid State **31**, 982 (1989)]; V. S. Bobrov, S. I. Zaitsev, and M. A. Lebedkin, Fiz. Tverd. Tela **32**, 3060 (1990) [Sov. Phys. Solid State **32**, 1176 (1990)].
[9] M. A. Lebyodkin, L. R. Dunin-Barkovskii, and T. A. Lebedkina, JETP Lett. **76**, 612 (2002).
[10] M. A. Lebyodkin, Y. Bréchet, Y. Estrin, and L. P. Kubin, Phys. Rev. Lett. **74**, 4758 (1995).
[11] C. Dunand-Châtellet, Ph.D. thesis, Ecole Polytechnique, France, 2012.
[12] J. Weiss, J.-R. Grasso, M.-C. Miguel, A. Vespignani, and S. Zapperi, Mater. Sci. Eng. A **309–310**, 360 (2001).
[13] J. Weiss, T. Richeton, F. Louchet, F. Chmelík, P. Dobroň, D. Entemeyer, M. Lebyodkin, T. Lebedkina, C. Fressengeas, and R. J. McDonald, Phys. Rev. B **76**, 224110 (2007).
[14] T. Richeton, P. Dobroň, F. Chmelík, J. Weiss, and F. Louchet, Mater. Sci. Eng. A **424**, 190 (2006).
[15] Y. Bougherira, D. Entemeyer, C. Fressengeas, N. P. Kobelev, T. A. Lebedkina, and M. A. Lebyodkin, J. Phys.: Conf. Series **240**, 012009 (2010).
[16] M. A. Lebyodkin, N. P. Kobelev, Y. Bougherira, D. Entemeyer, C. Fressengeas, V. S. Gornakov, T. A. Lebedkina, and I. V. Shashkov, Acta Mater. **60**, 3729 (2012).
[17] M. Zaiser, Adv. Phys. **55**, 185 (2006).
[18] D. M. Dimiduk, C. Woodward, R. LeSar, and M. D. Uchic, Science **312**, 1188 (2006).
[19] T. Richeton, J. Weiss, and F. Louchet, Nat. Mater. **4**, 465 (2005).
[20] I. V. Shashkov, M. A. Lebyodkin, and T. A. Lebedkina, Acta Mater. **60**, 6842 (2012).
[21] S. H. Strogatz, Phys. D: Nonlinear Phenom. **143**, 1 (2000).
[22] P. Bak, C. Tang, and K. Wiesenfeld, Phys. Rev. Lett. **59**, 381 (1987).
[23] J. P. Sethna, K. Dahmen, S. Kartha, J. A. Krumhansl, B. W. Roberts, and J. D. Shore, Phys. Rev. Lett. **70**, 3347 (1993).
[24] D. Sornette, Phys. Rev. Lett. **72**, 2306 (1994).
[25] P. Cizeau, S. Zapperi, G. Durin, and H. E. Stanley, Phys. Rev. Lett. **79**, 4669 (1997).
[26] G. Durin and S. Zapperi, Phys. Rev. Lett. **84**, 4705 (2000).
[27] R. A. White and K. A. Dahmen, Phys. Rev. Lett. **91**, 085702 (2003).
[28] F. J. Pérez-Reche, B. Tadić, L. Mañosa, A. Planes, and E. Vives, Phys. Rev. Lett. **93**, 195701 (2004).
[29] I. V. Shashkov, T. A. Lebedkina, M. A. Lebyodkin, P. Dobron, F. Chmelik, R. Kral, K. Parfenenko, and K. Mathis, Acta Phys. Pol. A **122**, 430 (2012).
[30] R. Král, P. Dobroň, F. Chmelík, V. Koula, M. Rydlo, and M. Janeček, Kovove Mater. **45**, 159 (2007).
[31] A. Vinogradov, D. L. Merson, V. Patlan, and S. Hashimoto, Mater. Sci. Eng. A **341**, 57 (2003).
[32] P. Rodriguez and S. Venkadesan, Solid State Phenom. **42-43**, 257 (1995).
[33] M. A. Lebyodkin, L. R. Dunin-Barkowskii,Y. Brechet, Y. Estrin, and L. P. Kubin, Acta Mater. **44**, 2529 (2000).
[34] H. D. I. Abarbanel, R. Brown, J. J. Sidorowich, and L. Sh. Tsimring, Rev. Mod. Phys. **65**, 1331 (1993).
[35] G. Ananthakrishna, C. Fressengeas, M. Grosbras, J. Vergnol, C. Engelke, J. Plessing, H. Neuhauser, E. Bouchaud, J. Planes, and L. P. Kubin, Scr. Metall. Mater. **32**, 1731 (1995).
[36] G. Ananthakrishna, Phys. Rep. **440**, 113 (2007).
[37] J. Gauthier, P. R. Louchez, and F. H. Samuel, Cast Met. **8**, 107 (1995).
[38] G. Pickering, J. M. Bull, and D. J. Sanderson, Tectonophysics **248**, 1 (1995).
[39] A. Clauset, C. Shalizi, and M. Newman, SIAM Rev. **51**, 661 (2009).
[40] K. Mathis and F. Chmelik, in *Acoustic Emission*, edited by W. Sikorsky (InTech, Rijeka, 2012), p. 23.
[41] J. Baró, Á. Corral, X. Illa, A. Planes, E. K. H. Salje, W. Schranz, D. E. Soto-Parra, and E. Vives, Phys. Rev. Lett. **110**, 088702 (2013).
[42] L. Laurson, X. Illa, and M. J. Alava, J. Stat. Mech.-Theory Exp. (2009) P01019.